Contact-implicit Trajectory and Grasp Planning for Soft Continuum Manipulators

Moritz A. Graule[1*], Clark B. Teeple[1], Robert J. Wood[1]

***Abstract*— As robots begin to move from structured industrial environments to the real world, they must be equipped to not only safely interact with the environment, but also reason about how to leverage contact to perform tasks. In this work, we develop a modeling and motion planning framework for continuum robots that accounts for contact anywhere along the robot. We first present an analytical model for continuum manipulators under contact and discuss the ideal choice of generalized coordinates given properties of the manipulator and task specifications. We then demonstrate the utility of our model by developing a motion planning framework that can solve a diverse set of tasks. We apply our framework to end effector path planning for a soft arm in an obstacle-rich environment, and grasp planning for soft robotic grippers, where contact can happen anywhere on the arm or gripper. Finally, we verify the utility of our model and planning framework by planning a grasp with a desired contact force for a soft antipodal gripper and testing this grasp in a hardware demonstration. Overall, our model and planning approach further enhance soft and continuum robots where they already excel: utilizing contact with the world to achieve their goals with a gentle touch.**

I. Introduction

Robots are increasingly moving from constrained, structured settings (e.g., assembly lines and warehouses) to less controlled environments (e.g., construction sites, hospitals, or our homes), where they can enhance human capabilities and assist in patient care or activities of daily living. In these unstructured settings, robots are required to operate reliably under uncertainty, share their workspace with human collaborators, and impart precisely controlled forces on fragile objects without damaging them. Today's industry-standard robots typically try to meet these requirements through motion plans that limit or eliminate contacts with their surroundings. However, as traditional robots tend to be both powerful and rigid, relying on active obstacle avoidance can be dangerous: perception or actuation system errors, or small disturbances can lead to vastly different contact interactions, and thus catastrophic failures that cause damage or injury.

Soft robots, in contrast to their rigid counterparts, can gently interact with the world despite failures or planning inaccuracies via passive compliance in their materials and/or structures [1]. Compliance has been leveraged in a variety of soft and continuum robotic manipulation systems spanning a broad range of applications, as summarized in Fig. 1. Soft hands have been developed for robust grasping of objects with uncertain properties [2]–[5], as well as in-hand manipulation [6]–[8]. Continuum arms can grasp objects with contact anywhere along their length (inspired by elephant trunks and octopus arms) [9], [10] without exceeding force thresholds. Soft arms have also been deployed as safe wearable devices to assist with lifting or holding items [11], have enabled workspace sharing or co-operation with humans [12], and were proposed for autonomously solving household tasks [13]. Continuum arms can also leverage their whole-body compliance to navigate unknown surroundings with ease [14]. This enables pick-and-place tasks in cluttered environments; exploration of rubble in search and rescue scenarios [15]; and medical applications such as organ retraction, and steering of endoscopes and

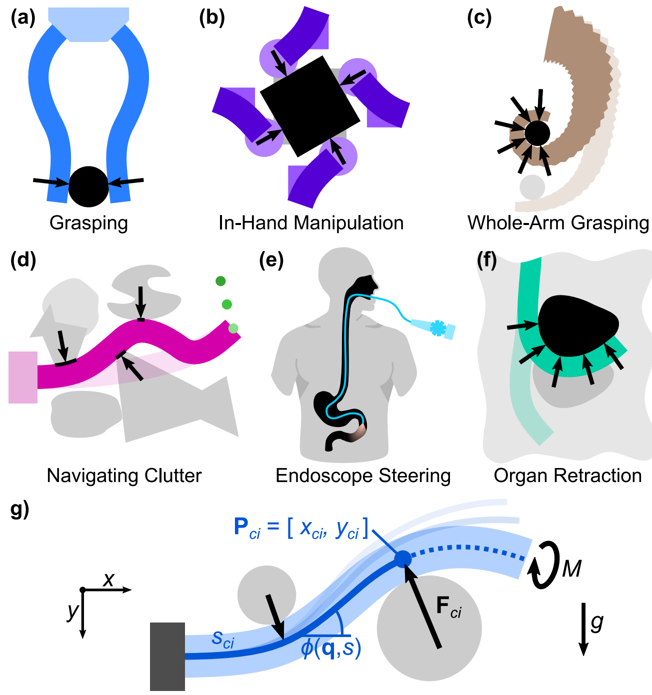

Fig. 1: Continuum robots are commonly applied to a variety of applications where contact with the world is key to success. a) Grasping, b) in-hand manipulation, and c) whole-arm grasping (as demonstrated by elephant trunks) can require contact along the entire length of manipulator. d) Navigating an end-effector through clutter, e) navigating an endoscope, and f) organ retraction during surgery can all be best performed by planning to utilize contact with the world (or human body). g) In this work, we present a model and path planning framework for continuum manipulators undergoing contact interactions with obstacles or objects in their environment. Our approach accounts for the effect of gravity in systems with a low or high stiffness-to-weight ratio, i contact forces $\mathbf{F_{ci}}$, and robot actuation torque M.

[1]John A. Paulson School of Engineering and Applied Sciences, Harvard University, 150 Western Avenue, Allston MA 02134, USA.

[*]Correspondence to `graulem@g.harvard.edu`

This material is based upon work supported by the National Science Foundation (award number EFMA-1830901); and a Space Technology Research Institutes grant (number 80NSSC19K1076) from NASA's Space Technology Research Grants Program. Any opinions, findings, conclusions, or recommendations expressed in this material are those of the authors and do not necessarily reflect those of the funding organizations.

needles [16]–[19].

Utilizing the compliance of soft systems, researchers have demonstrated impressive capabilities with either feed-forward control [20], [21] or planning and closed-loop control with the assumption that contact interactions are limited to the end-effector [22] or can be neglected altogether [14], [23]. Operating soft robots outside of an artificially-constrained laboratory setting, however, may necessitate accurate knowledge and control of their shape and contact interactions along their whole body. For example, in medical procedures, organ retraction requires a force sufficiently high to hold the organ but below the trauma threshold [18]. Similarly, forces cannot exceed damage thresholds in grasping and in-hand manipulation of delicate objects. In addition, whole-arm manipulation and pick-and-place operations can only be precisely executed if the effects of contact disturbances along the whole manipulator are accounted for.

The analytical model we present in this work addresses this need, accurately accounting for the influence of actuation torques, gravity, and an unlimited number of contact forces along the neutral axis (backbone) of a soft robotic manipulator. In summary, we make the following contributions:

- We present an analytical model for soft continuum manipulators that undergo contact interactions with obstacles or objects in their environment (Section III).
- We show how this model can be incorporated into a nonlinear program to enable contact-aware trajectory planning for soft robots.
- We showcase the capability of this planning framework by solving two cardinal tasks: navigating clutter with a soft arm that leverages bracing for improved accuracy (Section IV-A); and robust grasping of obstacles with varying diameters with a soft gripper (Section IV-B).
- We demonstrate the utility and accuracy of our grasp planner through simulations and an experimental validation on physical hardware (Sections V and VI).

II. Related Work

Soft robotic grasping and manipulation has traditionally relied on open-loop control of actuators with minimal modeling and planning involved, with the promise of passive adaptation to the environment. Many soft grippers forgo proprioception or force feedback entirely, with great success in simple tasks [2], [5]. However, without any explicit planning of contact forces, the stability of most grasps (while robust to uncertainties) are difficult to observe or predict. Grasp planning can be used to enable robots to choose how to place their soft fingers to achieve optimal grasps.

A variety of approaches exist for robust modeling and control of soft robots [24]. Many modeling frameworks assume the neutral axis of a soft manipulator follows a piecewise constant curvature shape [14], [25]. However, this model breaks down when the robot makes contact with the environment. In addition, Koopman operator theory has been successfully used to account for variation in payload mass to ensure accurate end effector trajectories [26]. These modeling frameworks are robust, but to date they have only considered contact at the end-effector, only indirectly modeling the effects of forces imparted along the arm [27].

Grasp planning, which has its roots in rigid mechanical systems, has been applied with limited success to soft robots. For example, the classical stability metric used in many grasp planners, epsilon quality, assumes perfectly rigid fingers [28]. This metric, and other relevant grasp quality measures, have been extended to include compliant contacts as well [29], [30]. More recently, learning-based approaches to grasp planning have shown great promise for rigid and soft robotic hands alike [31], [32]. However, these techniques can often produce spurious results in new situations, or require substantial computational power to obtain reasonable results.

Finally, trajectory planning where contact is explicitly accounted for is critical for applications such as manipulation and walking (where contact is essential). Trajectory planning with contact interactions is a nontrivial problem from the computational side [33]. Control of walking behavior heavily utilizes contact, which has required innovation in the problem formulation for optimization [34], [35]. For manipulation, contact modeling has also been a crucial area of study [36], as well as considering compliant contact in the planning process [37].

III. Analytical Model

A. Contact-implicit continuum robot dynamics

Here, we derive the equations of motion for a continuum manipulator experiencing contact with its environment. A detailed depiction of the system under consideration can be found in Fig. 1(g). The manipulator has length L and is controlled via a tip-applied moment M (e.g., from cable actuation). Let the manipulator configuration be described in general coordinates $\mathbf{q}$; different choices for generalized coordinates are discussed in Section III-C. Given generalized coordinates $\mathbf{q}$, we express the manipulator's backbone curve as a function of $\mathbf{q}$ and arc length s. The coordinates of a point along the backbone then are $(x(\mathbf{q},s), y(\mathbf{q},s))$, where

$$x(\mathbf{q},s) = \int_0^s \cos(\phi(\mathbf{q},\hat{s}))d\hat{s},$$

$$y(\mathbf{q},s) = \int_0^s \sin(\phi(\mathbf{q},\hat{s}))d\hat{s},$$

with backbone angle $\phi(\mathbf{q},s)$.

External contact forces $\mathbf{F_{ci}}$ act on the continuum robot at $(x(\mathbf{q},s_{ci}), y(\mathbf{q},s_{ci}))$. While the contact forces act perpendicular to the actuator's backbone (corresponding to a frictionless system) in our setup, our framework can be extended to allow contact forces within a pre-specified friction cone.

We can derive the governing equations for this continuum robot from the Euler-Lagrange equation:

$$\frac{d}{dt}\left(\frac{\partial \mathscr{L}}{\partial \dot{\mathbf{q}}}\right) - \frac{\partial \mathscr{L}}{\partial \mathbf{q}} = \tau - \mathbf{b}^T\dot{\mathbf{q}}. \quad (1)$$

This includes the Lagrangian $\mathscr{L} = T - V$ (with kinetic energy T and potential energy V), generalized forces τ, and the generalized damping term $\mathbf{b}^T\dot{\mathbf{q}}$. The potential energy V stored in this system consists of energy from backbone

TABLE I: Continuum manipulator deformation models for $n = 3$ generalized coordinates

	Piecewise constant curvature (PCC)	**Piecewise smooth curvature (PSC)**
generalized coordinates	curvature of three segments with lengths l_1, l_2, l_3	coefficients of 3rd order Legendre polynomial
backbone curvature ω	$\begin{cases} q_1 & \text{if } s \leq l_1 \\ q_2 & \text{if } s \leq l_1 + l_2 \\ q_3 & \text{if } s \leq l_1 + l_2 + l_3 \end{cases}$	$\frac{q_1}{L} + \frac{q_2}{L}\left(\frac{2s}{L} - 1\right) + \frac{q_3}{L}\left(\frac{6s^2}{L^2} - \frac{6s}{L} + 1\right)$
backbone angle $\phi(\mathbf{q}, s)$	$\begin{cases} q_1 s & \text{if } s \leq l_1 \\ q_1 l_1 + q_2(s - l_1) & \text{if } s \leq l_1 + l_2 \\ q_1 l_1 + q_2 l_2 + q_3(s - l_1 - l_2) & \text{if } s \leq l_1 + l_2 + l_3 \end{cases}$	$q_1 \frac{s}{L} + q_2\left(\frac{s^2}{L^2} - \frac{s}{L}\right) + q_3\left(\frac{2s^3}{L^3} - \frac{3s^2}{L^2} + \frac{s}{L}\right)$
curvature energy V_c	$\sum_i \frac{EI}{2} l_i q_i^2$	$\frac{EI}{2L}\left(q_1^2 + \frac{q_2^2}{3} + \frac{q_3^2}{5}\right)$
tip angle $\phi_t(\mathbf{q})$	$\sum_i l_i q_i$	q_1

curvature V_c, backbone extension V_e, gravitational energy V_g, and, depending on actuator type, fluid pressure or cable tension; its kinetic energy T is due to the velocity of the backbone's mass T_{kin} and, for fluidic actuation, fluid flow.

Ignoring the effect of fluid flow, the system's kinetic energy can be obtained as:

$$T_{kin} = \frac{1}{2}\int_0^L \rho(s)\left(\dot{x}(\mathbf{q}, s)^2 + \dot{y}(\mathbf{q}, s)^2\right) ds,$$

with $\rho(s)$ being the manipulator's linear density as a function of s. The components of the potential energy can be expressed in generalized coordinates as:

$$V_c = \frac{EI}{2}\int_0^L \kappa(\mathbf{q}, s)^2 ds,$$

$$V_e = \frac{EA_e}{2}\Delta L^2,$$

$$V_g = g\int_0^L \rho(s) y(\mathbf{q}, s) ds,$$

where I is the moment of inertia of the continuum manipulator, E its effective Young's modulus, κ its backbone curvature, A_e its effective area, ΔL its change in backbone length, and g indicates gravity acting in negative y-direction.

Given a number of i contact points $\mathbf{P_{ci}} = [x(s_{ci}), y(s_{ci})]^T = [x_{ci}, y_{ci}]^T$ along the manipulator, with contact forces $\mathbf{F}_{ci} = F_{ci}[\sin(\phi_{ci}), -\cos(\phi_{ci})]^T$, and a tip moment M, the generalized forces can be expressed as:

$$\tau = \sum_i J_{ci}^T \mathbf{F}_{ci} + \frac{\partial \phi_t}{\partial \mathbf{q}} M.$$

Here, J_{ci} indicates the Jacobian that transfers the contact forces at point $\mathbf{P_{ci}}$ into generalized forces (see [38] for more details); ϕ_t is the tip angle. The Jacobian J_{ci} is computed as:

$$J_{ci} = \frac{\partial \mathbf{P_{ci}}}{\partial \mathbf{q}}.$$

B. Simplifying assumptions

Throughout the remainder of this paper, we make a number of assumptions to simplify the equations governing the continuum manipulator's behavior. Many soft robots are designed to mostly deform along a primary bending axis, exhibiting significantly higher stiffness in resistance to forces perpendicular to this axis. We therefore restrict the bending beam deformations to lie within the primary bending plane and neglect the effect of torsion and transverse shear forces. We limit our treatment to quasi-static applications and also assume the actuator to be inextensible (which is accurate for many cable driven and pneumatic actuator designs). Without loss of generality, we consider only one contact interaction along the manipulator and ignore the effect of friction.

C. Generalized coordinates

The selection of generalized coordinates used to express the manipulator's backbone configuration affects the accuracy and computational complexity of the model. The ideal choice for generalized coordinates can depend on the application and the physical properties of the continuum manipulator. A common choice is the Piecewise Constant Curvature (PCC) model [39], in which each actuator is split into n segments of constant length; the curvatures of these segments are then chosen as the generalized coordinates. Benefits of this approach are conceptual simplicity, and high accuracy in specific load cases: given a static bending beam with neither a distributed load, nor compressive or shear forces applied, the solution to the static Euler-Bernoulli differential equation, which describes the deformation of a bending beam under simplifying assumptions (i.e., small deflections and linear elasticity), is a beam with constant curvature.

For more complex load cases, however, a different representation of the manipulator's backbone shape may be better suited. Generally speaking, one can pick n functions from an orthogonal set of basis functions (e.g., trigonometric or polynomial functions) to approximate each segment of the manipulator, and use the coefficients of this representation as the generalized coordinates. Odhner et al. introduced the Piecewise Smooth Curvature (PSC) model, which leverages Legendre polynomials as basis functions, and demonstrated that this choice achieves significantly higher accuracy than the PCC model for complex load cases [38].

We provide implementations of our model and path planning framework in both the PCC and the PSC coordinates. The expressions of key components of our model in both coordinate systems are listed in Table I for $\dim(\mathbf{q}) = 3$. For reasons outlined above, the PSC representation is better suited for soft robots under complex load cases (i.e., experiencing contact forces along their backbone). We further believe that the PSC representation is the appropriate choice for continuum arms with a low stiffness-to-weight ratio, as the distributed load in this case has a non-negligible effect on manipulator configuration, leading to deformations with non-constant curvature. Therefore, the results presented in Sections V and VI leverage the PSC assumption.

IV. Problem Formulation

We addressed the two problems of planning for a desired end-effector position for an arm navigating an environment with an obstacle (Section V-A), and planning for a desired manipulator configuration, contact force magnitude, and contact force direction in soft antipodal grasping (Section V-B). We formulated these two tasks as constrained nonlinear programs that share the same general structure (shown in Equation 2), but vary in their objective function $f(\mathbf{x})$ and decision variables $\mathbf{x}$:

$$\begin{array}{lrcll} & \min_{\mathbf{x}} & f(\mathbf{x}) & & \\ \text{s.t.} & h_e(\mathbf{q}) & = & 0 & \\ & \Phi(\mathbf{q}, s_{check}) & \leq & 0 & \forall s_{check} \\ & \Phi(\mathbf{q}, s_c) & \leq & 0 & \\ & -\mathbf{F_c} \cdot (\mathbf{P}_c - \mathbf{P}_o) & \leq & 0 & \\ & \Phi(\mathbf{q}, s_c) F_c - \lambda & = & 0 & \\ & -\lambda & \leq & 0 & \\ & |M| & \leq & M_{max} & \\ & 0 & \leq & F_c & \leq \; F_{max} \\ & 0 & \leq & s_c & \leq \; L. \end{array} \tag{2}$$

At the heart of both optimization problems lies a constraint that enforces a feasible state based on Equation 1 as:

$$\frac{d}{dt}\left(\frac{\partial \mathscr{L}}{\partial \dot{\mathbf{q}}}\right) - \frac{\partial \mathscr{L}}{\partial \mathbf{q}} - \tau + \mathbf{b}^T \dot{\mathbf{q}} = 0. \tag{3}$$

In the steady-state simplification (i.e., $\dot{\mathbf{q}} = 0$) and assuming actuation with moment M_a at the tip, we can derive the equality constraint $h_e(q) = 0$ from Eq. 3 as:

$$h_e(\mathbf{q}) := \frac{\partial \mathscr{L}(\mathbf{q})}{\mathbf{q}} + \sum_i J_{ci}^T \mathbf{F}_{ci} + \frac{\partial \phi_t}{\partial q} M. \tag{4}$$

The constraints further contain non-penetration constraints with guard function $\Phi(\mathbf{q}, s)$ that ensure that the manipulator does not penetrate the obstacle; a constraint enforcing that the contact force $\mathbf{F}_c$ points away from the obstacle ($-\mathbf{F}_c \cdot (\mathbf{P}_c - \mathbf{P}_o) \leq 0$); and a complementarity constraint ($\Phi(\mathbf{q}, s_c) F_c - \lambda = 0$) which ensures that contact forces can only be non-zero when the contact point lies on the obstacle and the manipulator.

The guard function $\Phi(\mathbf{q}, s) = -||\mathbf{P}_s - \mathbf{P}_o||_2 + r_o$ is a function of the obstacle's radius r_o and position $\mathbf{P}_o = [x_o, y_o]^T$, as well as a point $\mathbf{P}_s = (x_s, y_s)$ on the manipulator at arc length s. It is evaluated at N_{check} equally spaced check points s_{check} along the backbone to ensure that no point of the manipulator lies inside the obstacle region ($N_{check} = 20$ provided sufficient performance), and at the contact point at s_c. A slack variable λ is introduced in the complementarity constraint to improve the convergence behavior of the optimization; this variable, initialized to relax the constraint at the start of the optimization process, is eventually driven to zero through a dedicated term in the objective function ($\beta_1 \lambda$). Finally, we limit the magnitude of the actuation torque and contact force to M_{max} and F_{max} respectively, and constrain s_c to lie on the manipulator.

A. Quasi-static pose planning

In this setting, we plan for a manipulator configuration that brings the end-effector as close as possible to a desired pose (position and orientation, designated as $\mathbf{P}_{t,d}$). We introduce a circular obstacle into our planning environment, with which the manipulator is not allowed to overlap. The obstacle is defined by its center coordinates $[x_o, y_o]$ and its radius r_o. We optimize over the actuation torque applied at the tip ($u = M$), one contact force with magnitude (F_c) and position along the curve (s_c), and the manipulator configuration ($\mathbf{q}$). We solve this task through the nonlinear program outlined in Eq. 2; the complete objective function for this problem is shown below in Eq. 5, followed by an explanation of its terms:

$$f(\mathbf{x}) = u^T R u + (\mathbf{P}_{t,d} - \mathbf{P}_t)^T Q (\mathbf{P}_{t,d} - \mathbf{P}_t) + (\mathbf{P}_o - \mathbf{P}_c)^T Q_c (\mathbf{P}_o - \mathbf{P}_c) + \beta_1 \lambda - \beta_2 F_c. \tag{5}$$

This objective penalizes the magnitude of actuation torques ($u^T R u$) and the deviation from the desired tip pose ($(\mathbf{P}_{t,d} - \mathbf{P}_t)^T Q (\mathbf{P}_{t,d} - \mathbf{P}_t)$). A term rewarding proximity between the contact point on the backbone and the obstacle ($(\mathbf{P}_o - \mathbf{P}_c)^T Q_c (\mathbf{P}_o - \mathbf{P}_c)$) is included. R, Q, and Q_c are positive semi-definite and can be adjusted depending on the relative importance of the respective objective terms. As outlined earlier, the cost function also contains a term with a slack variable ($\beta_1 \lambda$, with $\beta_1 \geq 0$) to relax the contact complementarity constraint ($\Phi(\mathbf{q}, s_c) F_c$). A term rewarding higher contact forces ($\beta_2 F_c$, with $\beta_2 \geq 0$) can be added to the cost in order to drive the convergence towards solutions utilizing contact.

B. Grasp planning

In this demonstration, we plan antipodal pinch grasps for two soft fingers as illustrated in Fig. 2. Each of the fingers consists of two independently actuated segments in series, based on the design presented in [5]. We aim to plan a symmetrical grasp for a cylindrical object with center coordinates $[x_o, y_o]$ and radius r_o such that the contact forces are maximized, while no net forces are imparted on the object. We formulate this task as a nonlinear program with the structure and constraints introduced in Eq. 2 and the following objective:

$$f(\mathbf{x}) = \mathbf{F_c}^T \mathbf{a_{sym}} + (\mathbf{P}_o - \mathbf{P}_c)^T Q_c (\mathbf{P}_o - \mathbf{P}_c) + \beta_1 \lambda - \beta_2 F_c. \tag{6}$$

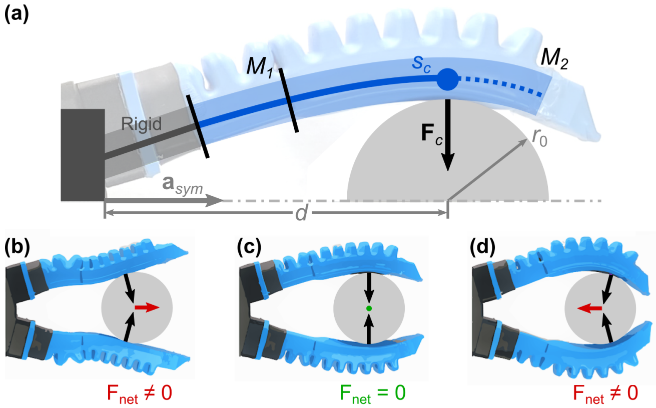

Fig. 2: We demonstrate the capability to plan symmetrical antipodal grasps for soft fingers with two pneumatic actuator segments per finger. (a) We plan for the direction and magnitude of the contact force F_c that the soft fingers (blue) exert onto a cylindrical object (grey) with radius r_o. A plan prescribes the torques M_1 and M_2 applied to the proximal and distal segments of the fingers, as well as the distance between the palm and the object center (d). (b-d) The objective of our grasp planner is to find settings for M_1, M_2, and d that achieve a sufficiently strong grasping force without imparting a net force onto the object to minimize the risk of unexpected object motion (and thus grasp failure).

This objective function contains a term that projects the contact force onto the gripper's axis of symmetry (which has direction $\mathbf{a_{sym}}$). Minimizing this term (while simultaneously maximizing the contact force magnitude F_c) penalizes grasps that impart a destabilizing force onto the object (net force F_{net} in Fig. 2(b-d)). The remaining terms of the objective function were introduced and explained in Section IV-A.

We assume that the two fingers receive identical control commands. We optimize over the fingers' proximal and distal actuation torques (M_1 and M_2, respectively), the manipulator configuration ($\mathbf{q}$), the contact force magnitude (F_c) and location (s_c), as well as the distance between the gripper base and the obstacle (d). Optionally, d can be constrained to be within a desired range $[d_{min}, d_{max}]$.

V. Simulation Results

In this section, we showcase how our framework can be used to plan for intricate contact interactions between continuum robots and their environment. First, we quantify the end-effector positioning error and required actuation torque for a large number of target positions in four different planning scenarios in which the obstacle is either absent, avoided, or used for bracing. We then demonstrate the ability to plan a trajectory that leverages bracing against an obstacle to minimize the distance between desired and achieved end-effector position. We compare the resulting trajectory to trajectories planned without an obstacle and ones planned to strictly avoid contact with the obstacle. Finally, we show how our model can be used to accurately plan for the direction and magnitude of contact forces in grasps with compliant fingers. For all these cases, we solve the respective nonlinear programs (as introduced in Section IV) using SNOPT [40].

A. Planning end-effector placement

In order to demonstrate the utility of our framework and highlight the importance of accurately modeling contact interactions that soft continuum robots undergo with their environment, we present a comparison of end-effector placement planning under four distinct paradigms: (i) planning and plan execution in the absence of obstacles; (ii) planning under the assumption that no obstacle is present, followed by plan execution in the presence of an obstacle; (iii) planning and plan execution in the presence of an obstacle, such that no contact occurs (i.e., traditional 'obstacle avoidance'); and (iv) planning and plan execution in the presence of an obstacle, explicitly allowing and planning for contact interactions between robot and obstacle. While planning under paradigms (i)-(iii) is feasible with traditional models for continuum manipulators, our model is uniquely suited to plan under paradigm (iv). The herein presented framework enables planning for end-effector placements, robot configurations, and/or desired contact forces under all four paradigms through changes to the constraints defining the minimum and maximum allowed contact force. We demonstrate this capability by planning for a set of desired end-effector positions (Fig. 3, green) in each of the paradigms on a toy problem with one obstacle. The manipulator in this setting consists of one actuator.

We further highlight how our framework can be used to accurately plan for bracing against obstacles to extend a soft robot's reachable space under strict torque limits. This is of particularly importance for soft robotic arms, which are often restricted in reachability and end-effector force output by their low relative strength. We show plans obtained under a high ($M_{max} = 10\,\mathrm{N\,mm}$, Fig. 3(a-d)) and low ($M_{max} = 2.5\,\mathrm{N\,mm}$, Fig. 3(e-h)) torque limits.

Manipulator and – if present – obstacle geometry and placement were held constant across all runs, while the desired end-effector position was varied. The same 25 end-effector goal positions, shown in Fig. 3(a-h) in green, were planned for in each of the paradigms for each torque limit. The decision variable initialization was identical across runs and chosen such that the initial guess for the manipulator configuration describes a manipulator passing the obstacle on the upper side. For each target end-effector position, we found the optimal configuration and torque commands by solving the nonlinear program described in Eq. 5, recording the final torque command and end-effector positioning error. Mean and standard deviation of required torques and resulting contact forces and positioning errors across the 25 runs for each paradigm and torque limit are shown in Fig. 3. These results show that planning under paradigm (iv) achieves the lowest average errors, and demonstrate how our framework can provide motion plans that leverage bracing, which is of great benefit for soft arms with strict actuation limits. Specifically, the weaker manipulator is not strong enough to remain above the obstacle without contacting it. The manipulator therefore passes above the obstacle under planning paradigm (ii) (causing a non-zero contact force), and underneath the obstacle in the obstacle-avoidance paradigm (which prevents contact forces but results in high positioning errors). Conversely, under planning paradigm (iv), the manipulator exploits its ability to make contact with

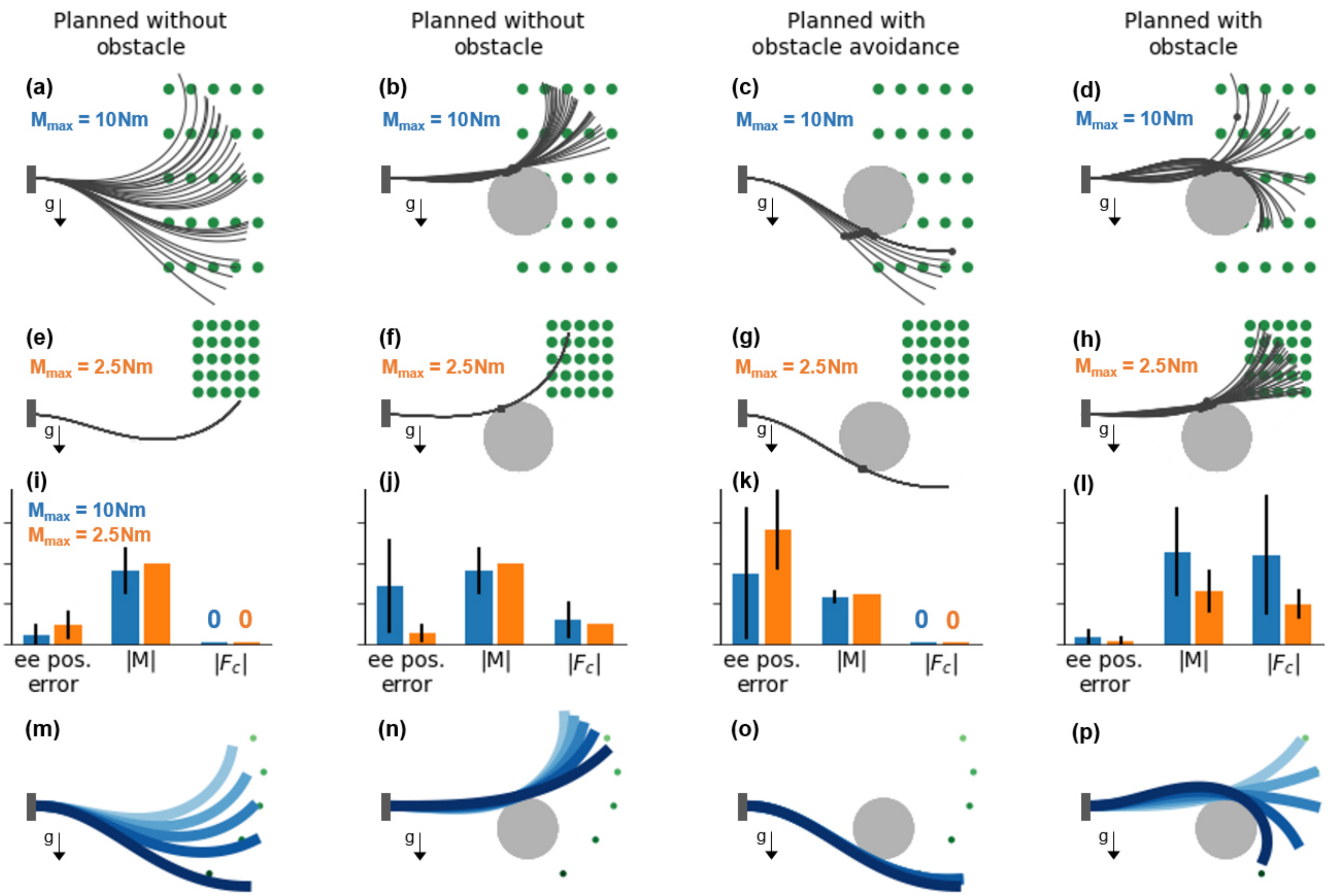

Fig. 3: We compare traditional path planning paradigms for soft arms (columns 1-3) to our contact-implicit approach (column 4). (a-d) A continuum arm with one actuator is tasked to reach a target (green) without exceeding an actuation limit of $M_{max} = 10\,\mathrm{N\,m}$. Configurations were planned separately for the 25 different end-effector targets shown in green. (e-h) The same arm is tasked to reach the goal positions shown in green, but it is now limited to a torque below $M_{max} = 2.5\,\mathrm{N\,m}$. (i-l) We show the mean actuation required, as well as the average end-effector positioning errors and contact forces for the previously introduced planning tasks for high (blue) and low (orange) torque limits. (m-p) For each of the planning paradigms, we plan a quasi-static trajectory in which the arm attempts to track a series of end-effector goal positions (from light to dark green). The resulting arm configurations are shown in light to dark blue.

its environment to bring the end-effector closer to its target.

In addition to the quantitative evaluation of planning end-effector placement under the different paradigms described above, we illustrate the capability to plan quasi-static end-effector trajectories in each of the paradigms. In these experiments, we prescribe a trajectory of desired tip positions (see Fig. 3(m-p), green), and solve our path planning nonlinear program for these goal positions. For each time step, the nonlinear program is initialized with the solution of the previous time step to accelerate the search for a feasible solution and to encourage solutions that are close to the previous solution. The resulting trajectories for each of the planning paradigms are shown in Fig. 3(m-p). As expected, the end-effector is able to track the target trajectory reasonably well under paradigms (i) and (iv), shown in Fig. 3(m) and Fig.3(p), respectively. Higher tracking errors are evident in the plans obtained under paradigms (ii) and (iii), depicted in Fig. 3(n) and Fig.3(o), respectively.

B. Grasp planning

Planning for the magnitude and direction of the forces that soft fingers impart on an object in a two-finger pinch grasp is beneficial for two reasons: the stability, robustness, and strength of a two-finger pinch grasp is affected by the direction and magnitude of the applied forces; and prescribing precise limits on the magnitude of the contact force prior to grasp execution facilitates gentle interactions between a gripper and fragile objects. The ability to prescribe a series of known contact forces between continuum fingers and an object is further useful in planning in-hand manipulation sequences with soft robotic hands.

We show that our framework can be used to plan for a desired direction and magnitude of a contact force between a soft robotic finger and an object by planning a two-fingered pinch grasp. In our setting, each of the pneumatically actuated continuum fingers has two segments for which the bending torques can be controlled independently (similar to the hardware described in [5]). Given an object with diameter d, we set up a nonlinear program to obtain the actuation torques and the relative position between the gripper's palm and the object such that the net force imparted by the two fingers is zero, while the magnitude of each contact force is maximized (within predefined bounds). We plan grasps for object diameters ranging from 15 mm to 70 mm;

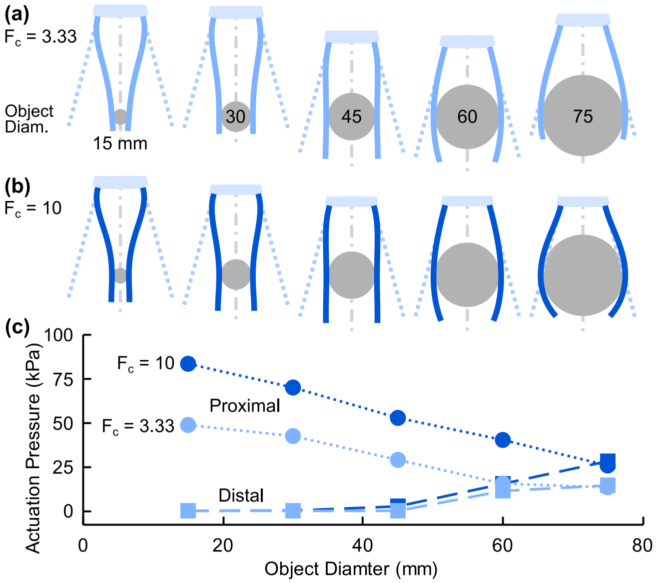

Fig. 4: Implementing contact force limits on objects leads to different planned grasps for optimal stability. Grasps were planned for cylindrical objects ranging from 15 mm to 75 mm diameter with a contact force limit of a) $F_c = 3.33$ N and b) $F_c = 10$ N. c) The planned actuation pressures are shown for each case.

for each object, we plan two grasps, one each with a low ($F_{max} = 10$ N) and high ($F_{max} = 3.3$ N) contact force limits. The planned control inputs and resulting grasp configurations are visualized in Fig. 4.

VI. Hardware Validation

To demonstrate the capabilities of our analytical model and grasp planning framework, we validate the ability to robustly grasp an object with a desired force on physical hardware. We used a pneumatically-powered soft gripper with two independently-actuated bending segments per finger (first demonstrated in [5]) with symmetric control of the fingers. After calibrating the planner with measured lengths (each finger is 100 mm long, where the distal segment is 30% of the the total length) and stiffnesses (EI), a grasp was planned for a desired maximum contact force of 3.3 N on a table-mounted cylindrical object with a diameter of 60 mm. The physical gripper then grasps a sensorized object at the planned actuation pressures and centering position. The sensorized object is constructed from two half-cylinders which are each rigidly attached to an ATI Nano17 six-axis load cell, both of which are fixed to mechanical ground. This enables measurement of forces and torques imparted on the object during grasping.

A sketch of the planned grasp, overlayed on a photo of the grasp's execution in hardware, is shown in Fig. 5(top). We observe good agreement in the resulting grasping force when applying the planned actuation torques to the hardware system (see Fig. 5(b)). The planner attempts to achieve contact forces pointing directly toward the object's center of mass which results in an optimal grasp. However, if sub-optimal grasps are performed, a net destabilizing force is imparted on the sensorized cylinder. To validate this in hardware, we investigated the resulting destabilizing forces for sub-optimal distal segment pressures, as shown in Fig. 5(a,b). As expected, when the distal segment is weakened, the object is pushed away from the gripper, while a stronger distal segment forces the object toward the gripper's palm. This illustrates the importance of our grasp planning approach in obtaining actuator torques and gripper positions that lead to contact forces that maximize grasp strength and stability.

VII. Conclusion and Outlook

In this work, we developed an analytical model and associated motion planning framework for continuum robots under contact with obstacles or objects anywhere along their length, and discussed how the properties of the manipulator and task specifications inform the choice of generalized coordinates. Based on our model, we then developed a motion planning framework to solve several important tasks: contact force estimation, end-effector path planning, and grasp planning. Finally, through a hardware demonstration, we verified the utility of our model by planning and executing grasps with a desired contact force.

In the future, a variety of exciting pathways exist to expand this work. First and foremost, extending the model to three-dimensions is key to planning more interesting behaviors with 3D manipulators. Next, incorporating the dynamics of continuum manipulators into the model will enable dynamic motion planning. Additionally, estimation of contact from backbone shapes using an extended Kalman filter or similar framework could enable implicit contact sensing, a useful tool for control of soft systems.

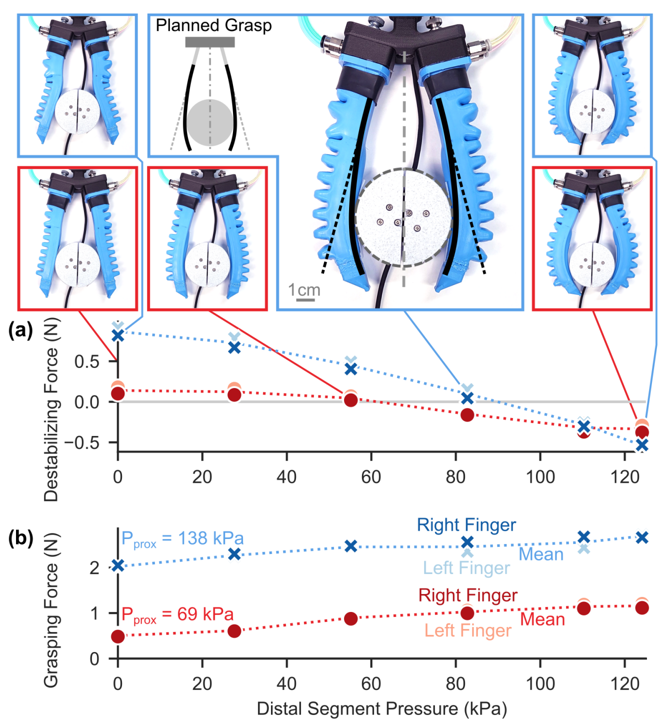

Fig. 5: Validation of the proposed modeling and planning framework applied to grasp planning. We plan one grasp (sketched) and execute it on hardware. We then sweep across different actuation torques in hardware that are sub-optimal, while measuring a) the destabilizing force applied to the object and b) the "grasping" force on the object. This shows the importance of grasp planning to ensure contact forces on the object lead to the best grasp.

REFERENCES

[1] D. Rus and M. T. Tolley, “Design, fabrication and control of soft robots,” *Nature*, vol. 521, no. 7553, p. 467, 2015.

[2] R. Deimel and O. Brock, “A novel type of compliant and underactuated robotic hand for dexterous grasping,” *The International Journal of Robotics Research*, vol. 35, no. 1-3, pp. 161–185, 2016.

[3] L. U. Odhner, L. P. Jentoft, M. R. Claffee, N. Corson, Y. Tenzer, R. R. Ma, M. Buehler, R. Kohout, R. D. Howe, and A. M. Dollar, “A compliant, underactuated hand for robust manipulation,” *The International Journal of Robotics Research*, vol. 33, no. 5, pp. 736–752, 2014.

[4] J. Shintake, V. Cacucciolo, D. Floreano, and H. Shea, “Soft robotic grippers,” *Advanced Materials*, p. 1707035, 2018.

[5] C. B. Teeple, T. N. Koutros, M. A. Graule, and R. J. Wood, “Multi-segment soft robotic fingers enable robust precision grasping,” *The International Journal of Robotics Research*, vol. 39, no. 14, pp. 1647–1667, 2020.

[6] M. Liarokapis and A. M. Dollar, “Deriving dexterous, in-hand manipulation primitives for adaptive robot hands,” in *2017 IEEE/RSJ International Conference on Intelligent Robots and Systems (IROS)*. IEEE, 2017, pp. 1951–1958.

[7] S. Abondance, C. B. Teeple, and R. J. Wood, “A dexterous soft robotic hand for delicate in-hand manipulation,” *IEEE Robotics and Automation Letters*, vol. 5, no. 4, pp. 5502–5509, 2020.

[8] A. Bhatt, A. Sieler, S. Puhlmann, and O. Brock, “Surprisingly robust in-hand manipulation: An empirical study-supplementary material,” in *Robotics Science and Systems Conference (RSS)*, 2021.

[9] N. G. Cheng, M. B. Lobovsky, S. J. Keating, A. M. Setapen, K. I. Gero, A. E. Hosoi, and K. D. Iagnemma, “Design and analysis of a robust, low-cost, highly articulated manipulator enabled by jamming of granular media,” in *2012 IEEE International Conference on Robotics and Automation*, 2012, pp. 4328–4333.

[10] C. Laschi, M. Cianchetti, B. Mazzolai, L. Margheri, M. Follador, and P. Dario, “Soft robot arm inspired by the octopus,” *Advanced robotics*, vol. 26, no. 7, pp. 709–727, 2012.

[11] D. Prattichizzo, M. Pozzi, T. L. Baldi, M. Malvezzi, I. Hussain, S. Rossi, and G. Salvietti, “Human augmentation by wearable supernumerary robotic limbs: review and perspectives,” *Progress in Biomedical Engineering*, vol. 3, no. 4, p. 042005, sep 2021.

[12] P. H. Nguyen, I. I. Mohd, C. Sparks, F. L. Arellano, W. Zhang, and P. Polygerinos, “Fabric soft poly-limbs for physical assistance of daily living tasks,” in *2019 International Conference on Robotics and Automation (ICRA)*. IEEE, 2019, pp. 8429–8435.

[13] J. Fathi, T. J. O. Vrielink, M. S. Runciman, and G. P. Mylonas, “A deployable soft robotic arm with stiffness modulation for assistive living applications,” in *2019 International Conference on Robotics and Automation (ICRA)*. IEEE, 2019, pp. 1479–1485.

[14] A. D. Marchese, R. K. Katzschmann, and D. Rus, “Whole arm planning for a soft and highly compliant 2d robotic manipulator,” in *2014 IEEE/RSJ International Conference on Intelligent Robots and Systems*. IEEE, 2014, pp. 554–560.

[15] E. W. Hawkes, L. H. Blumenschein, J. D. Greer, and A. M. Okamura, “A soft robot that navigates its environment through growth,” *Science Robotics*, vol. 2, no. 8, p. eaan3028, 2017.

[16] T. Ranzani, G. Gerboni, M. Cianchetti, and A. Menciassi, “A bioinspired soft manipulator for minimally invasive surgery,” *Bioinspiration & biomimetics*, vol. 10, no. 3, p. 035008, 2015.

[17] I. De Falco, M. Cianchetti, and A. Menciassi, “A soft multi-module manipulator with variable stiffness for minimally invasive surgery,” *Bioinspiration & biomimetics*, vol. 12, no. 5, p. 056008, 2017.

[18] A. Melzer, G. Buess, and A. Cuschieri, “Instrumentation and allied technology for endoscopic surgery,” in *Operative Manual of Endoscopic Surgery 2*. Springer, 1994, pp. 1–69.

[19] N. Mehta, R. Haluck, M. Frecker, and A. Snyder, “Sequence and task analysis of instrument use in common laparoscopic procedures,” *Surgical Endoscopy And Other Interventional Techniques*, vol. 16, no. 2, pp. 280–285, 2002.

[20] K. C. Galloway, K. P. Becker, B. Phillips, J. Kirby, S. Licht, D. Tchernov, R. J. Wood, and D. F. Gruber, “Soft robotic grippers for biological sampling on deep reefs,” *Soft robotics*, vol. 3, no. 1, pp. 23–33, 2016.

[21] S. Kurumaya, B. T. Phillips, K. P. Becker, M. H. Rosen, D. F. Gruber, K. C. Galloway, K. Suzumori, and R. J. Wood, “A modular soft robotic wrist for underwater manipulation,” *Soft robotics*, vol. 5, no. 4, pp. 399–409, 2018.

[22] C. Della Santina, R. K. Katzschmann, A. Bicchi, and D. Rus, “Model-based dynamic feedback control of a planar soft robot: trajectory tracking and interaction with the environment,” *The International Journal of Robotics Research*, vol. 39, no. 4, pp. 490–513, 2020.

[23] D. Bruder, B. Gillespie, C. D. Remy, and R. Vasudevan, “Modeling and control of soft robots using the koopman operator and model predictive control,” *arXiv preprint arXiv:1902.02827*, 2019.

[24] C. Della Santina, C. Duriez, and D. Rus, “Model based control of soft robots: A survey of the state of the art and open challenges,” *arXiv preprint arXiv:2110.01358*, 2021.

[25] C. Della Santina, R. K. Katzschmann, A. Biechi, and D. Rus, “Dynamic control of soft robots interacting with the environment,” in *2018 IEEE International Conference on Soft Robotics (RoboSoft)*. IEEE, 2018, pp. 46–53.

[26] D. Bruder, X. Fu, R. B. Gillespie, C. D. Remy, and R. Vasudevan, “Koopman-based control of a soft continuum manipulator under variable loading conditions,” *IEEE Robotics and Automation Letters*, vol. 6, no. 4, pp. 6852–6859, 2021.

[27] R. K. Katzschmann, A. D. Marchese, and D. Rus, “Autonomous object manipulation using a soft planar grasping manipulator,” *Soft robotics*, vol. 2, no. 4, pp. 155–164, 2015.

[28] C. Ferrari and J. F. Canny, “Planning optimal grasps.” in *ICRA*, vol. 3, no. 4, 1992, p. 6.

[29] M. Ciocarlie and P. Allen, “A design and analysis tool for underactuated compliant hands,” in *2009 IEEE/RSJ International Conference on Intelligent Robots and Systems*. IEEE, 2009, pp. 5234–5239.

[30] M. Pozzi, M. Malvezzi, and D. Prattichizzo, “On grasp quality measures: Grasp robustness and contact force distribution in underactuated and compliant robotic hands,” *IEEE Robotics and Automation Letters*, vol. 2, no. 1, pp. 329–336, 2016.

[31] C. Choi, W. Schwarting, J. DelPreto, and D. Rus, “Learning object grasping for soft robot hands,” *IEEE Robotics and Automation Letters*, vol. 3, no. 3, pp. 2370–2377, 2018.

[32] I. Akkaya, M. Andrychowicz, M. Chociej, M. Litwin, B. McGrew, A. Petron, A. Paino, M. Plappert, G. Powell, R. Ribas *et al.*, “Solving rubik’s cube with a robot hand,” *arXiv preprint arXiv:1910.07113*, 2019.

[33] D. Stewart and J. C. Trinkle, “An implicit time-stepping scheme for rigid body dynamics with coulomb friction,” in *Proceedings 2000 ICRA. Millennium Conference. IEEE International Conference on Robotics and Automation. Symposia Proceedings (Cat. No. 00CH37065)*, vol. 1. IEEE, 2000, pp. 162–169.

[34] U. Muico, Y. Lee, J. Popović, and Z. Popović, “Contact-aware nonlinear control of dynamic characters,” in *ACM SIGGRAPH 2009 papers*, 2009, pp. 1–9.

[35] M. Posa, C. Cantu, and R. Tedrake, “A direct method for trajectory optimization of rigid bodies through contact,” *The International Journal of Robotics Research*, vol. 33, no. 1, pp. 69–81, 2014.

[36] N. Chavan-Dafle and A. Rodriguez, “Sampling-based planning of in-hand manipulation with external pushes,” in *Robotics Research*. Springer, 2020, pp. 523–539.

[37] C. Guan, W. Vega-Brown, and N. Roy, “Efficient planning for near-optimal compliant manipulation leveraging environmental contact,” in *2018 IEEE International Conference on Robotics and Automation (ICRA)*. IEEE, 2018, pp. 215–222.

[38] L. U. Odhner and A. M. Dollar, “The smooth curvature model: An efficient representation of euler–bernoulli flexures as robot joints,” *IEEE Transactions on Robotics*, vol. 28, no. 4, pp. 761–772, aug 2012.

[39] R. J. Webster III and B. A. Jones, “Design and kinematic modeling of constant curvature continuum robots: A review,” *The International Journal of Robotics Research*, vol. 29, no. 13, pp. 1661–1683, 2010.

[40] P. E. Gill, W. Murray, and M. A. Saunders, “Snopt: An sqp algorithm for large-scale constrained optimization,” *SIAM review*, vol. 47, no. 1, pp. 99–131, 2005.